Available online at www.sciencedirect.com
ScienceDirect
Trans. Nonferrous Met. Soc. China 34(2024) 171−183
Transactions of Nonferrous Metals Society of China
www.tnmsc.cn

In-situ preparation of high oxygen content titanium via wire arc additive manufacturing with tunable mechanical properties

Chang-yuan LI[1], Chang-meng LIU[1], Tao LU[1], Yue-ling GUO[1], Bin LIU[2]

1. School of Mechanical Engineering, Beijing Institute of Technology, Beijing 100081, China;
2. Beijing Institute of Astronautical Systems Engineering, China Academy of Launch Vehicle Technology, Beijing 100076, China

Received 15 July 2022; accepted 12 April 2023

Abstract: High oxygen content titanium (HOC-Ti) was manufactured in-situ via wire arc additive manufacturing (WAAM), and its compositional segregation, microstructure and mechanical properties were studied. The results show that the microstructure of the HOC-Ti component is mainly manifested as acicular α colonies. As oxygen content increases, the acicular α of the sample is broadened and the colonies become larger. Due to the strengthening of oxygen and the grain size effect, the strength change trend is from high to low, and the elongation is reduced significantly. The fracture mechanism is changed from ductile rupture to cleavage fracture. When the oxygen content is 0.37 wt.%, its elongation is about 7%, and the ultimate tensile strength is more than 730 MPa, which is around double that of commercially pure titanium (CP-Ti).

Key words: wire arc additive manufacturing; pure titanium; high oxygen content; microstructure; mechanical properties

1 Introduction

Because of their excellent properties such as high specific strength, high toughness, low density and exceptional creep, titanium and titanium alloys are widely applied in aerospace, etc. However, there are still some problems of titanium and titanium alloys, such as high cost of raw materials and difficulties of machining. Therefore, the preparation method of titanium alloys with low costs and excellent properties has always been one of the hot spots [1,2].

Oxygen is known to have a substantial hardening effect when residing in Ti matrix as interstitial atom [3−6]. YU et al [7] elucidated the origin of such strengthening effect, which was associated with repulsion created by the core of screw dislocation for oxygen. It is previously thought that the oxygen content should be limited to prevent it from embrittlement [7−9]. However, recent studies about powder metallurgy (PM) methods showed that commercially pure titanium (CP-Ti) with high oxygen and nitrogen contents has both high strength and tensile elongation [10−16]. CHEN et al [10] took the initiative to adding oxygen via PM. The alloy gained an ultimate tensile strength over 1000 MPa and an elongation to failure over 20%. LUO et al [15] studied the biocompatibility and mechanical properties of the high oxygen content titanium (HOC-Ti), which were better than those of CP-Ti. However, PM method needs to add oxygen by grinding or mixing rutile powder before long-time sintering. This can cause various limitations in actual production including poor efficiency and high costs. Besides, selective laser melting (SLM) has been proven to be useful in HOC-Ti preparing. The mechanical

Corresponding author: Chang-meng LIU, Tel/Fax: +86-10-68915097, E-mail: liuchangmeng@bit.edu.cn
DOI: 10.1016/S1003-6326(23)66389-7

properties were close to those of the PM method, though the powder was still used [17,18]. These works inspired us that adding interstitial elements like oxygen through additive manufacturing (AM) might be an efficient way to gain titanium alloys with low cost.

Wire arc additive manufacturing (WAAM) is one of the promising methods of metallic additive manufacturing. It uses electric arc as heat source to melt metallic wires, which can fabricate near-net-shape components. The advantages such as low costs, high deposition rate and high material utilization make it promising in industrial fabricating, especially for components with large size and complex geometry [19−21]. During the in-situ manufacturing process in the air, WAAM can add oxygen by the diffusion when melting CP-Ti wire. Ideally, the composition can also be uniform due to the point-by-point deposition. There is also less waste of materials and limitation in component size. Hence, it is more efficient and cheaper than PM method, which might be more proper in HOC-Ti preparation.

In previous studies [22,23], the oxidation of titanium alloys during WAAM is considered to be harmful. To prevent fabricated components from oxidation, a chamber filled with insert gas like argon or tracing shielding devices to form a volume region filled with inert gas is necessary [23−30]. Both require large amounts of inert gas. ELMER et al [31] studied the influence of different fusion atmosphere on the composition of WAAM samples. The oxygen content of Ti−6Al−4V fabricated in air is 1.5 times that of the wire. The nitrogen content is 7 times that of the wire. CABALLERO et al [32] studied the influence of the fusion atmosphere and processing parameters on the oxidation behavior of Ti−6Al−4V during WAAM fabricating. The results show that the current and the width of the melting pool are the main factors affecting the thickness of the α case. It is an oxygen-rich region formed in the surface oxidation, which is always thought harmful [33−35]. And higher oxygen content of the fusion atmosphere comes with higher strength and lower elongation. But sample strength changes little when the oxygen content of the fusion atmosphere is less than 0.4 wt.%. ZHOU et al [36] found that the ratio of length to width for Ti−6Al−4V α lamellar increased when the oxygen level increased. As mentioned above, studies mainly aim to protect components from oxidation to ensure high manufacturing quality at present. There is a lack of studies that add oxygen actively to CP-Ti. Hence, whether the WAAM method is feasible in HOC-Ti preparation needs to be verified.

The purpose of this work is to investigate the feasibility of manufacturing HOC-Ti in situ based on WAAM. One CP-Ti component and several HOC-Ti components with different oxygen contents were fabricated by WAAM. To study the influence of oxygen, the composition, microstructure and mechanical properties were characterized to build the relationship among them.

2 Experimental

There were two parts in this experiment. Firstly, the fusion atmosphere was changed to study the influence of oxygen content. HOC-Ti and CP-Ti components were manufactured in air and argon gas, respectively. Secondly, manufacturing parameters were changed to gain HOC-Ti components with different oxygen contents. The composition, microstructure and mechanical properties were characterized to figure out the relationship among them and oxygen content. The details were as follows.

2.1 Wire arc additive manufacturing equipment

The WAAM equipment used in this work is shown in Fig. 1(a), and its schematic is shown in Fig. 1(b). It consisted of a gas tungsten arc welding (GTAW) equipment, a control system, a wire feeder, a working chamber, a three-axis CNC machine tool and a resistance power source. The system was controlled by a personal computer.

2.2 Fabrication of components in different fusion atmosphere

The CP-Ti wire used in this work (1.6 mm in diameter) was utilized to deposit onto the Ti−6Al−4V plates (150 mm × 150 mm × 5 mm in dimensions). Two thin-walled square components (about 50 mm long, 50 mm wide and 70 mm high) were fabricated, as shown in Fig. 2(a). They were built by the same manufacturing parameters and different fusion atmosphere (argon gas for CP-Ti, and air for HOC-Ti). The manufacturing parameters are summarized in Table 1.

As shown in Fig. 2(b), several cubic samples

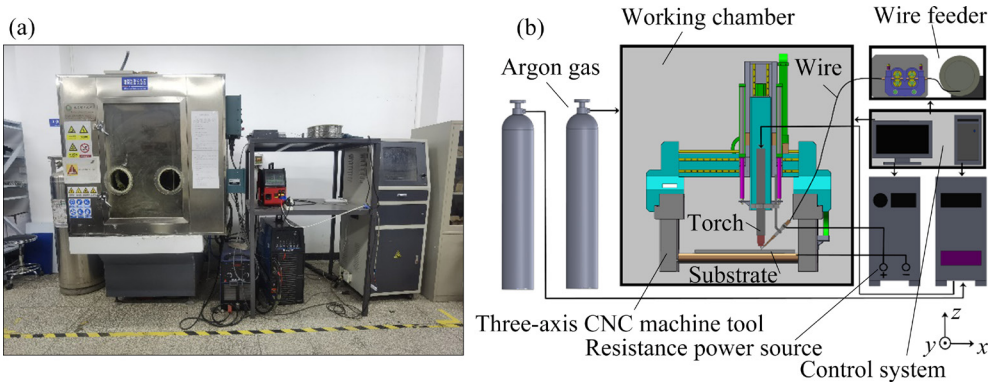

Fig. 1 Overview of wire arc addition manufacturing (WAAM) equipment (a), and schematic of equipment (b)

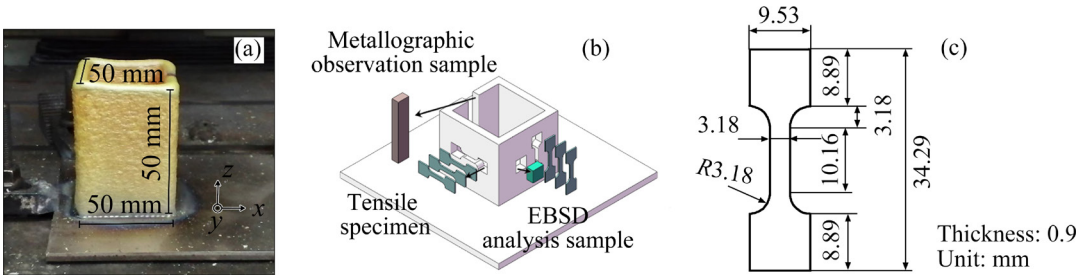

Fig. 2 Square component (a), sample preparation for testing (b), and dimension of tensile specimen (c)

Table 1 Manufacturing parameters of square components

Peak current/A	Base current/A	Peak current duration/%	Base current duration/%	Frequency/ Hz	Layer thickness/ mm	Wire feeding speed/ (cm·min^{-1})	Machine scanning speed/ (mm·min^{-1})
270	67.5	25	75	1.8	0.8	100	360

were taken from each component by electrical discharge machining (EDM). The vertical section of metallographic sample was ground by SiC grinding paper to 2000 grit size. Then it was polished by $3Fe_2O_3$−Cr_2O_3 slurry and etched by a mixed aqueous solution of 3 vol.% HF and 6 vol.% HNO_3. Besides, samples for electron backscattered diffraction (EBSD) of HOC-Ti and CP-Ti were prepared and then tested.

The size of the specimen is shown in Fig. 2(c). The tensile specimens were also extracted by EDM. They were executed at room temperature at a strain rate of 0.001 s^{-1}. Besides, the fracture surface of fractured tensile specimen was analyzed by scanning electron microscope (SEM). The broken tensile specimens were used as samples for chemical analysis. The mass fraction of oxygen, nitrogen and hydrogen were analyzed using inert gas fusion thermal infrared detection method.

2.3 Fabrication of components with different oxygen contents

The tensile testing result of HOC-Ti did not exceed our expectation, which showed great brittleness and might be affected by grain size effect. It has been proven that geometrical constraints strongly affect the impact of texture on mechanical properties anisotropy and fracture mechanisms in notched specimens [37]. And the structural stability of the specimens has influence on the overall ductility [37,38]. To get more accurate data, cylindroid tensile specimen was used as substitute. When considering the influence of α case and the allowance for machining, block part was fabricated to ensure the thickness. Compared with the square components, some changed details were as follows.

Several block parts (about 60 mm long, 45 mm wide and 45 mm high) were fabricated to study the influence of different oxygen contents. They were

all fabricated in air, as shown in Fig. 3(a). The block parts were all annealed for 1 h and cooled in air. The annealing temperature was not higher than 750 ℃, below the phase transformation temperature of Ti (882.5 ℃). Additionally, a resistance heat resistance power source was added, which was proven to have beneficial effect on the mechanical properties including grain refinement and decreasing the anisotropy [39].

To get different compositions, various combinations of manufacturing parameters were tried and three representative ones are listed in Table 2. Equations (1) and (2) were used to calculate the value of the average arc heat input [39]:

$$I_{av}=\frac{I_p t_p+I_b t_b}{t_p+t_b} \tag{1}$$

$$H_i=\eta I_{av}(V_{av}/S_T) \tag{2}$$

where I_{av} is the average current; V_{av} means the average voltage of GTAW; I_p is the peak current; I_b is the base current; t_p is the peak current duration and t_b is the base current duration; H_i is the average arc heat input; η is the welding efficiency which is about 0.83 for GTAW; S_T is the travel speed of the torch [40].

As shown in Fig. 3(b), strips (about 5 mm long and 5 mm wide) were cut by EDM to analyze the mass fraction of oxygen, nitrogen and hydrogen. The cubic sample (about 10 mm long and 10 mm wide) was also cut for metallographic observation. When considering the difference between the α case and the internal main part of the components, they were all cut in the central part. The dimension of the cylindroid tensile specimen is shown in Fig. 3(c). The fracture surface was also analyzed by SEM.

3 Results and discussion

3.1 Components fabricated in different fusion atmosphere

3.1.1 Chemical composition of HOC-Ti and CP-Ti

The mass fractions of oxygen, nitrogen and hydrogen of CP-Ti and HOC-Ti are given in Table 3. Compared with the CP-Ti, the oxygen and nitrogen contents of the HOC-Ti are obviously raised. The oxygen content is 0.31 wt.% higher. As for nitrogen, the content is increased by one order of magnitude. The result is foreseeable as titanium is sensitive to oxygen and nitrogen, especially at high temperatures. However, the hydrogen content is little changed, which is much lower than the critical hydrogen content of hydrogen-induced cracking and brittle hydrogen phase [41,42].

When considering the strength contribution from different elements, Eq. (3) can be used to convert the contents into equivalent oxygen content [16]. The equivalent oxygen content of HOC-Ti gained via WAAM is about 0.60 wt.%, and it is close to that of PM method, which is about 0.65 wt.% [15]. Hence, it is feasible to add oxygen and nitrogen through the diffusion when melting.

$$[O]_{Eq}=[O]+2[N] \tag{3}$$

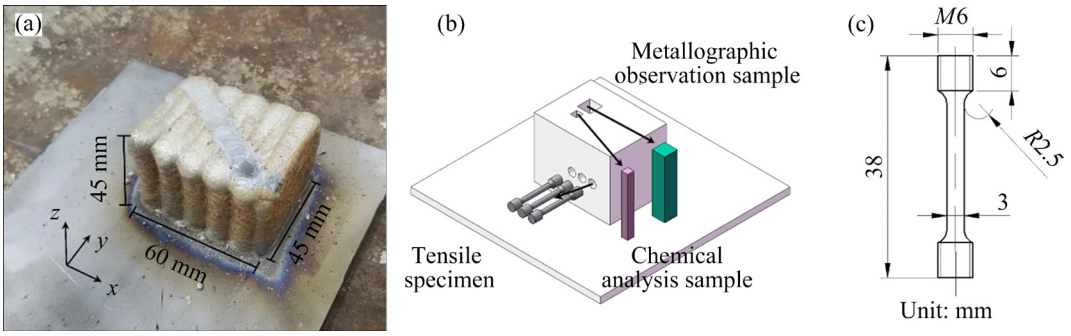

Fig. 3 One block part (a), sample preparation for testing (b), and dimension of tensile specimen (c)

Table 2 Manufacturing parameters of block parts

Average current/A	Average voltage/V	Layer thickness/mm	Wire feeding speed/ (cm·min^{-1})	Machine scanning speed/ (mm·min^{-1})	Oxygen content/ wt.%
155.9	14	2	200	330	0.17
167.5	14.5	2	200	330	0.37
201.3	15	2	200	300	0.48

Table 3 Contents of oxygen, nitrogen and hydrogen in CP-Ti and HOC-Ti (wt.%)

Fusion atmosphere	O	N	H	O (Equivalent)
Air	0.43	0.085	0.0031	0.60
Argon gas	0.12	0.0058	0.0039	0.13

3.1.2 Microstructure of HOC-Ti and CP-Ti

The OM images about the microstructure of HOC-Ti and CP-Ti are shown in Fig. 4. There are many colonies in HOC-Ti, which consist of a large amount of acicular α. Due to the influence of interstitial elements, crystal nucleus is formed mainly at the grain boundary. With the slow cooling and the low undercooling, grains grow from the boundary to the interior in parallel direction, forming the colonies of acicular α [43]. One single piece of colonies is large. The size can be even more than 2 mm. As for CP-Ti, the size of primary α colonies in CP-Ti is significantly smaller than that in HOC-Ti. And small phase is found in colonies (black area in Fig. 4(d)), which is thought to be secondary α related to the impurity like C [44].

Figure 5 shows the results of EBSD of HOC-Ti sample and CP-Ti sample. For HOC-Ti, the orientation in one single piece of colonies is almost the same because acicular α phases are all parallel. It was thought that α colonies determine the effective slip length, which affects the mechanical properties greatly [45]. Thus, one piece of colonies could be treated as a unit of deformation and fracture, which is similar to one single grain. The size of colonies is huge which is even more than 800 μm, resulting in a small ratio of sample size to grain size. Thus, the grain size effect is non-negligible as the properties of individual grains affect the deformation behavior significantly, which has a great effect on the mechanical properties [46].

As for CP-Ti, the grains are significantly smaller, as secondary α distributes in colonies and the primary α goes broken. The heat accumulation is significant in WAAM, the lower deposition zone is heated during the fabricating, which provides a similar effect like heat treatment [19]. This might be the reason why there appears secondary α. This also results in different orientations in the area, which is not proper to be treated as a single unit. The reason why there is no secondary α in HOC-Ti might be the stabilizing of oxygen.

3.1.3 Mechanical properties of HOC-Ti and CP-Ti

Figure 6 shows the average values of the ultimate tensile strength (UTS), yield strength (YS) and elongation (EL) of HOC-Ti and CP-Ti components fabricated separately in air and argon gas. The confidence interval was calculated using a 95% confidence level.

As shown in Fig. 6, the CP-Ti sample shows obvious plasticity. The ultimate tensile strength of specimens in longitudinal (L) direction is about 382 MPa, and the elongation is about 35%. The ultimate tensile strength of specimens in transversal (T) direction is about 396 MPa, and the elongation is about 42%. The tensile strength of T specimens is better than L specimens. The anisotropy in WAAM

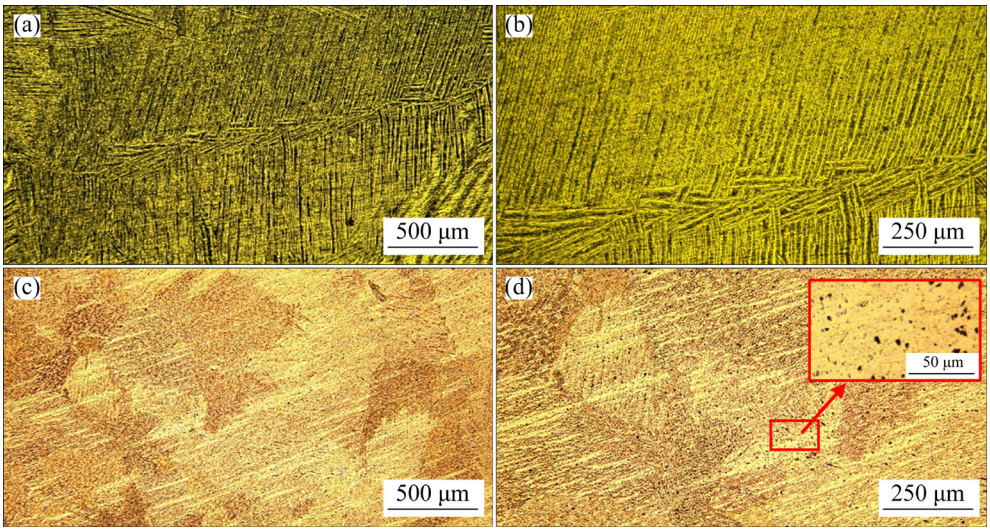

Fig. 4 Microstructure of HOC-Ti manufactured by WAAM in air (a, b) and microstructure of CP-Ti manufactured by WAAM in argon gas (c, d)

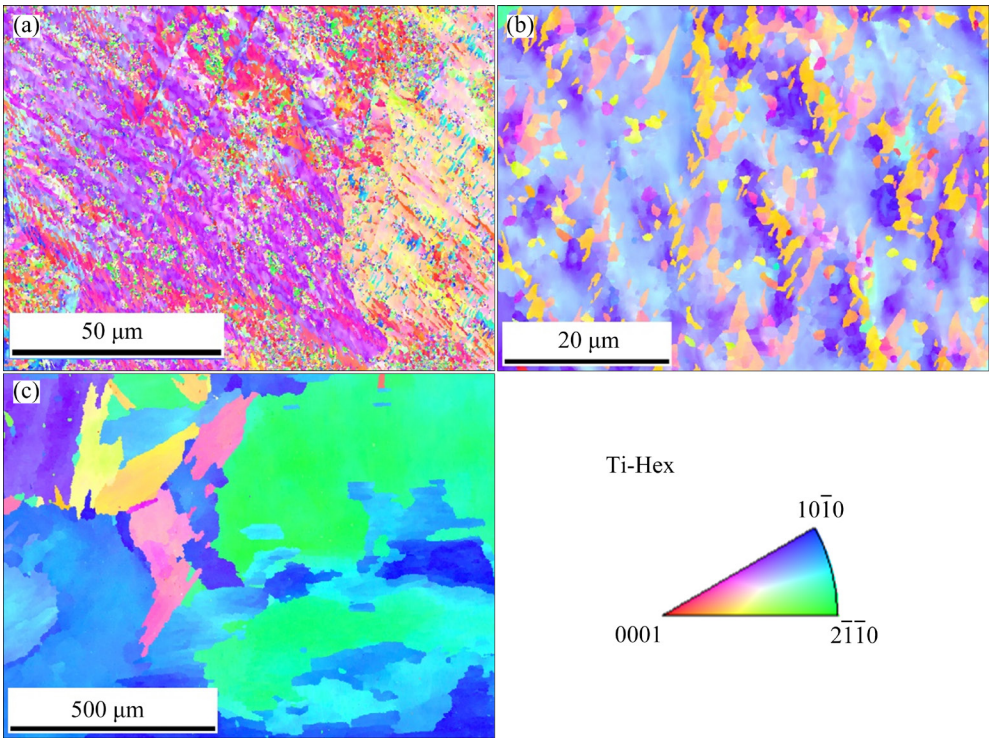

Fig. 5 EBSD analysis results of components manufactured by WAAM in different atmosphere: (a, b) HOC-Ti (90 nm in step size); (c) CP-Ti (1.75 μm in step size)

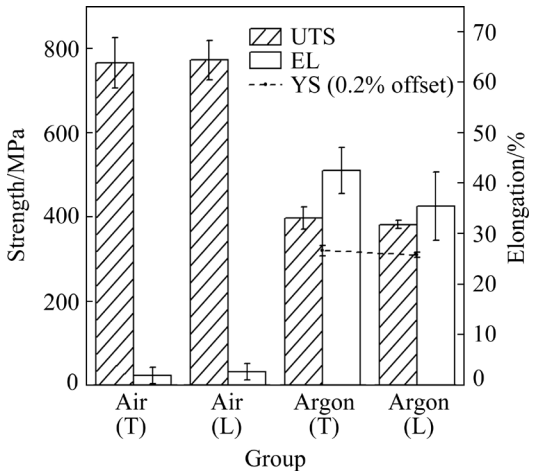

Fig. 6 Ultimate tensile strength (UTS), yield strength (YS) and elongation (EL) of HOC-Ti and CP-Ti components manufactured separately in air and argon gas (L−Longitudinal; T−Transversal)

was always thought to be related to the thermal gradient [19]. As grains grow along the build direction, less grain boundaries are observed in L direction, so the strength is lower. However, the reason of the decrease in elongation is uncertain. But similar results were also found in hot-rolled CP-Ti and electron beam [37,47,48]. It was explained that most deformation systems in specimens had no suitable position to form high accommodated strain in titanium grains [37,48]. WANG et al [47] explained it by the elongated pores in T direction, which tend to close up with load in T direction and open up with load in L direction. Figure 7(a) shows the macrostructure of the CP-Ti fracture, where there is obvious necking. And the SEM images of the microstructure are shown in Figs. 7(c, e). There are dimples of varying sizes, which conforms to the characteristics of ductile fracture.

As for HOC-Ti, the ultimate tensile strength of T specimens is about 766 MPa, and the elongation is about 1.9%. The ultimate tensile strength of L specimens is about 773 MPa, and the elongation is about 2.6%. The tensile strength of T specimens is slightly better than L specimens, and the anisotropy on mechanical properties is not significant. Compared with CP-Ti, the ultimate tensile strength increases by more than 360 MPa. The elongation decreases by more than one order of magnitude. The HOC-Ti sample manufactured in air shows great brittleness. Yielding can hardly be observed, so the yield strength is not marked in Fig. 6. The macrostructure of the HOC-Ti fracture is shown in Fig. 7(b), where there is no necking. And the micro-

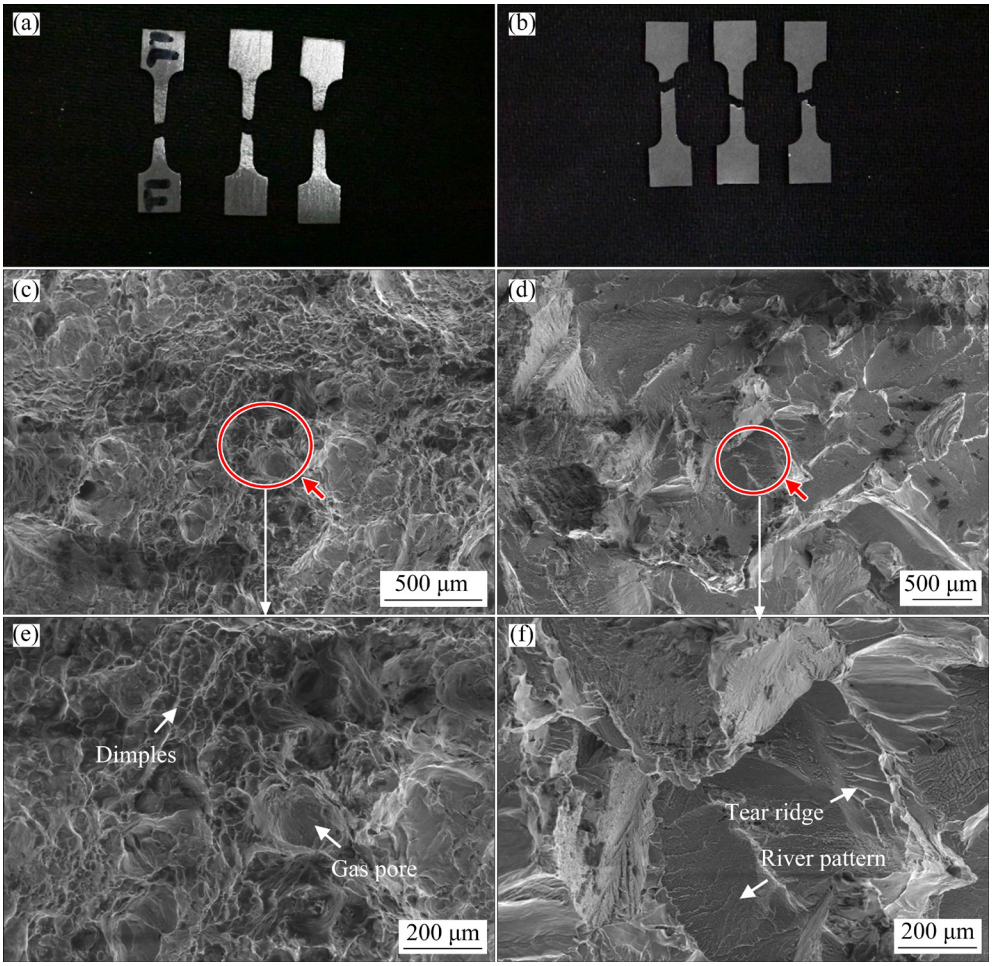

Fig. 7 Fracture morphologies of specimens: (a, c, e) CP-Ti; (b, d, f) HOC-Ti

structure of the HOC-Ti fracture is shown in Figs. 7(c, f). There are river patterns and several cleavages on the fracture, which conforms to the characteristics of brittle fracture.

The results can be connected to the micro-structure mentioned in Section 3.1.2. When fabricating in air, the oxygen absorbed stabilizes the α-Ti. This decreases the nucleation rate and is beneficial to the growth of acicular α. As acicular α phases are all parallel, one piece of colonies could be treated similar to a grain, which has single orientation. It has been proven that the grain size effect of titanium could cause the decrease in both elongation and strength [49,50]. The effect of large colonies size might be the reason of the significant decrease in elongation. But oxygen is also beneficial to the increase of strength, which has greater influence. Thus, the ultimate tensile strength is still improved. In addition, it is noticed that the average grain size of HOC-Ti manufactured by CHEN et al [10] can be less than 8 μm. The large extrusion ratio of PM method may play an important role, which is beneficial to the grain refinement and the compactness.

3.2 Titanium with different oxygen contents

3.2.1 Chemical composition of HOC-Ti with different oxygen contents

Figure 8 shows the relationship between average arc heat input (H_i) and mass fractions of oxygen, nitrogen and hydrogen. With the increase of the H_i, the content of oxygen and hydrogen increases observably. Higher temperature, larger contact area between molten pool and the air, and longer cooling time are beneficial to the gas proliferation, which can get higher oxygen and nitrogen content. However, the hydrogen content is basically stable, which may be the result of the low concentration and the weak gas proliferation of H_2 in the air.

According to a study about PM method, when the nitrogen content reaches 0.74 wt.%, the strength of the component is over 1120 MPa and the elongation is about 21.7% [51]. It seems that

nitrogen also has similar effect as oxygen because the data are clear for HOC-Ti [10]. When the equivalent oxygen content in HOC-Ti of WAAM is close to that of PM, the nitrogen content is not more than 0.2 wt.%, which is much lower than 0.74 wt.%. This means that oxygen still plays the main role.

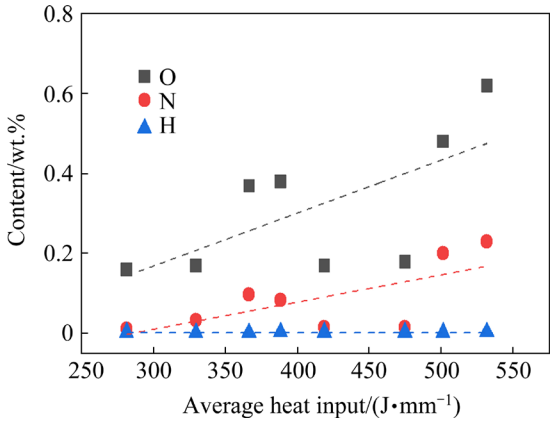

Fig. 8 Relationship between chemical composition (contents of oxygen, nitrogen and hydrogen) and average arc heat input

Additionally, due to the error accumulated in height during WAAM, the length of the arc between the tungsten electrode and the molten pool is ever-changing and hard to control. This is associated with the current and voltage, which means that the theoretical average heat input might be not accurate. Hence, how to achieve the accurate oxygen content regulation is still a problem.

3.2.2 Microstructure of HOC-Ti with different compositions

The OM images about the microstructure of the HOC-Ti with different oxygen contents are presented in Fig. 9. The average width (d_{av}) of acicular α was measured by the software ImageJ. The acicular α becomes wider and clearer with the increase of oxygen content. When the oxygen content is 0.17 wt.%, d_{av} is about 5.53 μm. But when the oxygen content reaches 1.10 wt.%, d_{av} is about 23.64 μm. The size of colonies also becomes larger. When the oxygen content is 0.17 wt.%, the colonies size is around 600 μm. But when the oxygen content reaches 1.10 wt.%, single piece of colonies is even beyond the scope of microscope observation, which is more than 1 cm.

The result can be explained by the fact that the α-Ti is stabilized by oxygen. The nucleation rate and density become lower with higher oxygen content, resulting in the increase of the acicular α width. As shown in Fig. 8, higher oxygen content always comes with higher heat input, which is also beneficial to the grain coarsening and forming larger colonies.

3.2.3 Mechanical properties of HOC-Ti with different compositions

The strain−stress curves of HOC-Ti with different oxygen contents are shown in Fig. 10. Different temperatures of annealing seem to have slight change in microstructure and properties.

As shown in Fig. 10, the mechanical properties change from plasticity to brittleness with the increase of oxygen content. The HOC-Ti shows good plasticity when the oxygen content is 0.17 wt.%. The ultimate tensile strength reaches 504 MPa. The yield strength reaches 420 MPa and

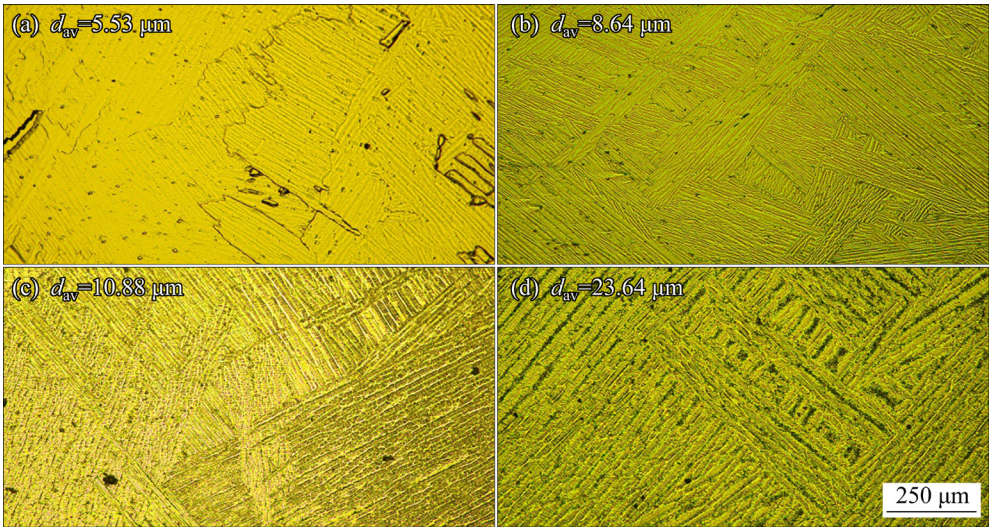

Fig. 9 Microstructures of HOC-Ti manufactured by WAAM with different oxygen contents: (a) 0.17 wt.%; (b) 0.48 wt.%; (c) 0.82 wt.%; (d) 1.10 wt.%

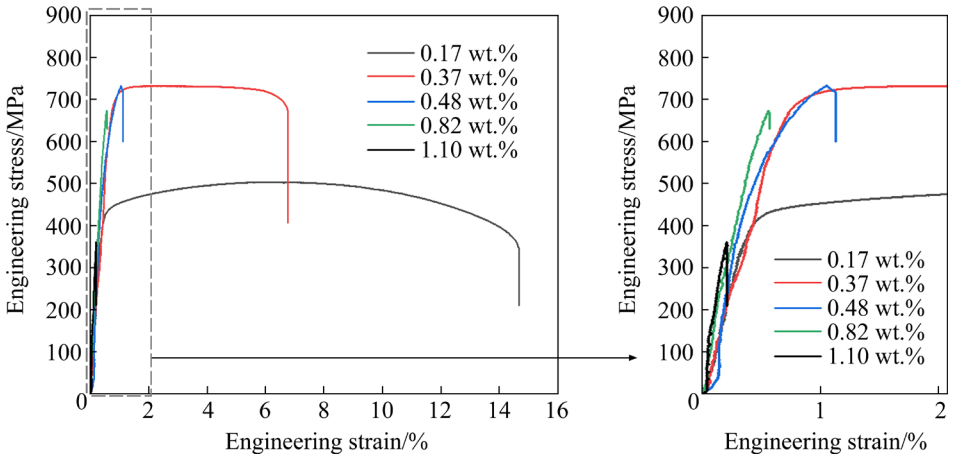

Fig. 10 Engineering stress−strain curves of HOC-Ti with different oxygen contents

the elongation is about 14.7%. When the oxygen content is 0.37 wt.%, there is a good balance of tensile strength and elongation of the HOC-Ti fabricated by WAAM. Its ultimate tensile strength is up to 732 MPa, yield strength is about 650 MPa, and elongation is about 6.7%. When the oxygen content is 0.48 wt.%, complete strain softening stage can hardly be observed, but there is still the strain strengthening stage. The ultimate tensile strength is about 733 MPa, but the elongation is only about 1.2%. When the oxygen content reaches 0.82 wt.%, the HOC-Ti shows completely brittleness with an elongation no more than 1%. Additionally, cracks and tipping occur more frequently due to the brittleness during machining. When the oxygen content reaches 1.10 wt.%, only one specimen is successfully machined, whose ultimate tensile strength is less than 400 MPa, and the elongation is about 0.3%.

The SEM images of the fractures are shown in Fig. 11. The fracture is gradually flattened with the increase of oxygen content. The forms of fracture change from ductile fracture to quasi-cleavage fracture and to cleavage fracture. When the oxygen content is 0.17 wt.%, it conforms to the characteristics of ductile fracture. There are many equiaxed dimples due to the nucleation, growth and aggregation of micro voids caused by the plastic deformation in micro range. When the oxygen content is 0.37 or 0.48 wt.%, the cleavage cracks come firstly and then are torn plastically, forming many tear ridges staggered and adhered with dimples and dimple bands, which conforms to the characteristics of quasi-cleavage fracture. When the oxygen is 0.82 wt.% or higher, characteristics of cleavage fracture such as river pattern and cleavage stage are more obvious, while dimples can be hardly seen. The forms of fractures turn to cleavage fracture at last.

The colonies mentioned in Section 3.2.2 explain the changes in mechanical properties of HOC-Ti well. When the oxygen content increases, the corresponding higher heat input causes coarse microstructure. The size of colonies is larger, resulting in more obvious grain size effect. Thus, there is a certain transition from plasticity to brittleness. This also explains the change in the strength. At first, the influence of grain size effect on the strength is weaker than the strengthening of oxygen. As colonies becomes larger, the grain size effect gradually increases and finally becomes the main factor. Hence, the ultimate tensile strength of HOC-Ti increases firstly and then decreases. So, how to get the equilibrium state is the priority. The oxygen content must be well-controlled as there is obvious connection between oxygen content and the size of acicular α colonies.

Compared with CP-Ti forgings according to ASTM B381, the tensile strength increases greatly. When the oxygen content is 0.37 wt.%, the tensile strength increases by more than one times, and the elongation is still receivable. What is the most important is that there is no need to prevent oxidation, which can leave out the huge gas cost and limitation in component size. As mentioned in Section 3.1.3, grain size effect brings worse elongation. Whether methods like cold rolling are helpful is a question, which is beneficial to the grain refinement. Hence, further studies are necessary to optimize WAAM method on HOC-Ti preparation.

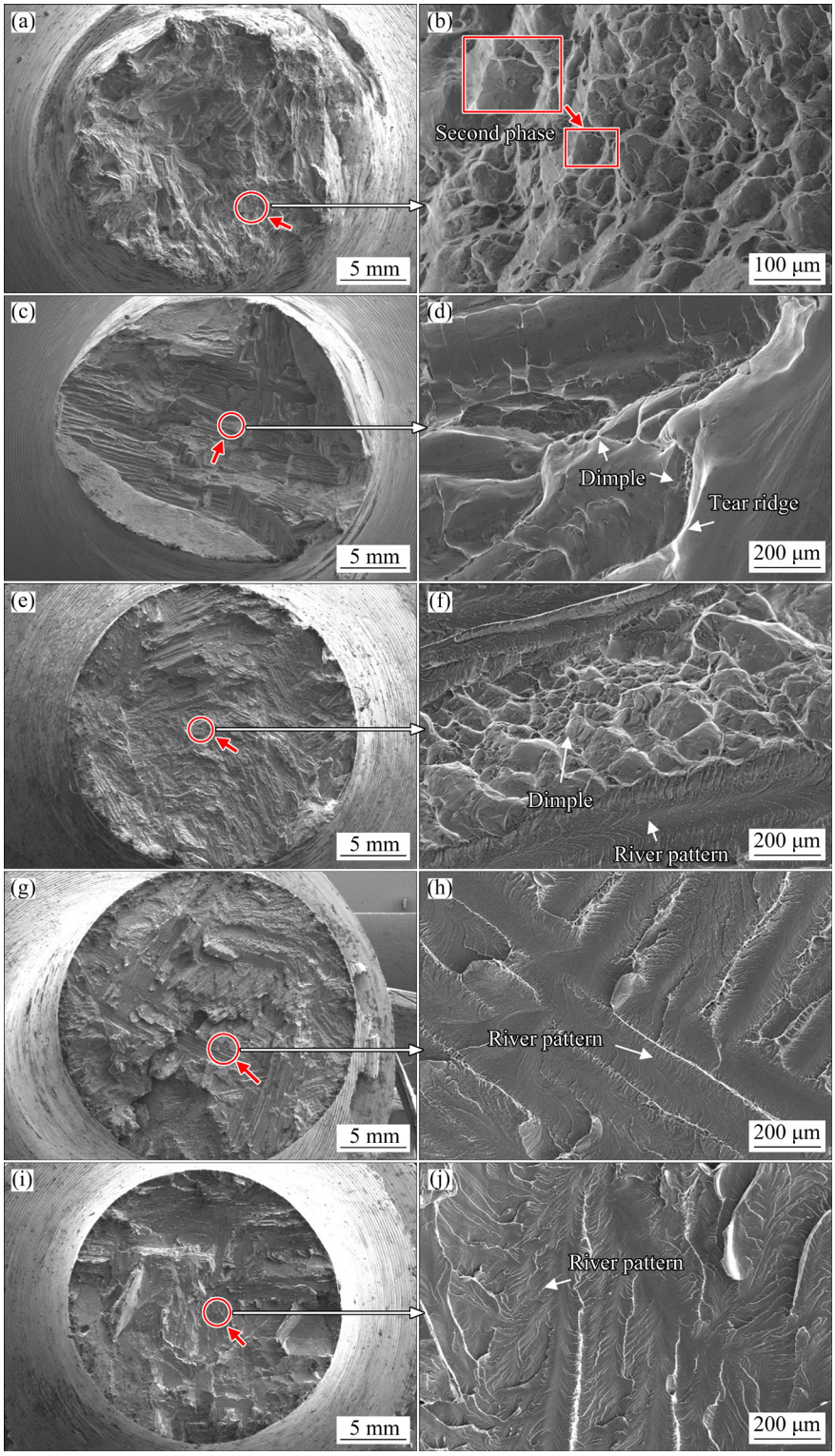

Fig. 11 Fracture morphologies of HOC-Ti with different oxygen contents: (a, b) 0.17 wt.%; (c, d) 0.37 wt.%; (e, f) 0.48 wt.%; (g, h) 0.82 wt.%; (i, j) 1.10 wt.%

4 Conclusions

(1) Compared with CP-Ti manufactured in argon gas, the oxygen and nitrogen contents of HOC-Ti manufactured in air are increased significantly, but the hydrogen content changes little. The oxygen content and nitrogen content increase with the increase of average arc heat input. But the hydrogen content changes little with the

increase of average arc heat input.

(2) Microstructure of HOC-Ti manufactured in air by WAAM is mainly manifested as acicular α colonies. Compared with HOC-Ti, the colonies size of CP-Ti manufactured in argon gas is smaller with secondary α distributing in it. When oxygen content increases, the width of acicular α is increased and colonies also become larger.

(3) Compared with the CP-Ti components manufactured in argon gas, the tensile strength of HOC-Ti components manufactured in air increases obviously. Meanwhile, the elongation reduces greatly. And the anisotropy in mechanical properties of CP-Ti is obvious, of which the strength in width direction is better. When the oxygen content increases, the mechanical properties of HOC-Ti change from plasticity to brittleness. The elongation reduces. The tensile strength increases firstly and then decreases. The form of fracture transits from ductile fracture to quasi-cleavage fracture and to cleavage fracture. When the oxygen content is 0.37 wt.%, the ultimate tensile strength of the alloy is more than 730 MPa. The yield strength is about 650 MPa, and the elongation (EL) is about 7%.

CRediT authorship contribution statement

Chang-yuan LI: Conceptualization, Investigation, Formal analysis, Writing − Original draft; **Chang-meng LIU:** Conceptualization, Funding acquisition, Resources, Supervision, Writing − Review & editing; **Tao LU:** Writing − Original draft, Writing − Review & editing; **Yue-ling GUO:** Writing − Review & editing; **Bin LIU:** Supervision.

Declaration of competing interest

The authors declare that they have no known competing financial interests or personal relationships that could have appeared to influence the work reported in this paper.

Acknowledgments

The work was financially supported by the National Natural Science Foundation of China (Nos. 51875041, 51875042).

References

[1] BODUNRIN M O, CHOWN L H, OMOTOYINBO J A. Development of low-cost titanium alloys: A chronicle of challenges and opportunities [J]. Materials Today: Proceedings, 2021, 38: 564−569.

[2] BANERJEE D, WILLIAMS J C. Perspectives on titanium science and technology [J]. Acta Materialia, 2013, 61(3): 844−879.

[3] CONRAD H. Effect of interstitial solutes on the strength and ductility of titanium [J]. Progress in Materials Science, 1981, 26(2/3/4): 123−403.

[4] OUCHI C, IIZUMI H, MITAO S. Effects of ultra-high purification and addition of interstitial elements on properties of pure titanium and titanium alloy [J]. Materials Science and Engineering A, 1998, 243: 186−195.

[5] LEFEBVRE L P, BARIL E, de CAMARET L. The effect of oxygen, nitrogen and carbon on the microstructure and compression properties of titanium foams [J]. Journal of Materials Research, 2013, 28(17): 2453−2460.

[6] WILLIAMS J C, SOMMER A W, TUNG P P. The influence of oxygen concentration on the internal stress and dislocation arrangements in α titanium [J]. Metallurgical and Materials Transactions B, 1972, 3(11): 2979−2984.

[7] YU Qian, QI Liang, TSURU T, TRAYLOR R, RUGG D, MORRIS J W, ASTA M, CHRZAN D C, MINOR A M. Origin of dramatic oxygen solute strengthening effect in titanium [J]. Science, 2015, 347(6222): 635−639.

[8] CHONG Yan, POSCHMANN M, ZHANG Ruo-peng, ZHAO Shi-teng, HOOSHMAND M S, ROTHCHILD E, OLMSTED D L, MORRIS JR J W, CHRZAN D C, ASTA M, MINOR A M. Mechanistic basis of oxygen sensitivity in titanium [J]. Science Advances, 2020, 6(43): c4060.

[9] XIA Yang, ZHAO Jin-long, TIAN Qing-hua, GUO Xue-yi. Review of the effect of oxygen on titanium and deoxygenation technologies for recycling of titanium metal [J]. JOM, 2019, 71(9): 3209−3220.

[10] CHEN Biao, SHEN Jiang-hua, YE Xiao-xin, UMEDA J, KONDOH K. Advanced mechanical properties of powder metallurgy commercially pure titanium with a high oxygen concentration [J]. Journal of Materials Research, 2017, 32(19): 3769−3776.

[11] KARIYA S, ISSARIYAPAT A, BAHADOR A, UMEDA J, SHEN Jiang-hua, KONDOH K. Ductility improvement of high-strength Ti−O material upon heteromicrostructure formation [J]. Materials Science and Engineering A, 2022, 842: 143041.

[12] CAI Ze-yun, XIANG Tao, ZHANG Zong-wei, BAO Wei-zong, CHEN Jia-yin, LI Bo-hua, XIE Guo-qiang. Enhancing the strength of pure titanium by the interstitial oxygen triggered dislocation motion [J]. SSRN Electronic Journal, 2022: 4075813.

[13] KONDOH K, SUN Bin, LI Shu-feng, IMAI H, UMEDA J. Experimental and theoretical analysis of nitrogen solid-solution strengthening of PM titanium [J]. International Journal of Powder Metallurgy, 2014, 50(3): 35−40.

[14] SUN Bin, LI Shu-feng, IMAI H, MIMOTO T, UMEDA J, KONDOH K. Fabrication of high-strength Ti materials by in-process solid solution strengthening of oxygen via P/M methods [J]. Materials Science and Engineering A, 2013, 563: 95−100.

[15] LUO Hui-wen, WU Yu-lu, DIAO Xiao-ou, SHI Wen-di, FENG Fan, QIAN Fei, UMEDA J, KONDOH K, XIN Hai-tao, SHEN Jiang-hua. Mechanical properties and biocompatibility of titanium with a high oxygen

concentration for dental implants [J]. Materials Science and Engineering C, 2020, 117: 111306.

[16] SHEN Jiang-hua, CHEN Biao, UMEDA J, KONDOH K. Microstructure and mechanical properties of CP-Ti fabricated via powder metallurgy with non-uniformly dispersed impurity solutes [J]. Materials Science and Engineering A, 2018, 716: 1−10.

[17] KONDOH K, ICHIKAWA E, ISSARIYAPAT A, SHITARA K, UMEDA J, CHEN Biao, LI Shu-feng. Tensile property enhancement by oxygen solutes in selectively laser melted titanium materials fabricated from pre-mixed pure Ti and TiO_2 powder [J]. Materials Science and Engineering A, 2020, 795: 139983.

[18] SHI Wen-di, YANG Ya-hui, KANG Nan, WANG Min-jie, CHEN Biao, LI Yu-long, UMEDA J, KONDOH K, SHEN Jiang-hua. Microstructure and mechanical characterizations of additively manufactured high oxygen-doped titanium [J]. Materials Characterization, 2022, 189: 112008.

[19] LIN Zi-dong, SONG Kai-jie, YU Xing-hua. A review on wire and arc additive manufacturing of titanium alloy [J]. Journal of Manufacturing Processes, 2021, 70: 24−45.

[20] LIN Zi-dong. Wire and arc additive manufacturing of thin structures using metal-cored wire consumables: Micro-structure, mechanical properties, and experiment-based thermal model [D]. Delft University of Technology, 2019.

[21] WILLIAMS S W, MARTINA F, ADDISON A C, DING Jia-luo, PARDAL G, COLEGROVE P. Wire + arc additive manufacturing [J]. Materials Science and Technology, 2016, 32(7): 641−647.

[22] QI Yun-lian, DENG Ju, HONG Quan, ZENG Li-ying. Electron beam welding, laser beam welding and gas tungsten arc welding of titanium sheet [J]. Materials Science and Engineering A, 2000, 280: 177−181.

[23] BERMINGHAM M J, THOMSON-LARKINS J, ST JOHN D H, DARGUSCH M S. Sensitivity of Ti−6Al−4V components to oxidation during out of chamber wire + arc additive manufacturing [J]. Journal of Materials Processing Technology, 2018, 258: 29−37.

[24] POUZET S, PEYRE P, GORNY C, CASTELNAU O, BAUDIN T, BRISSET F, COLIN C, GADAUD P. Additive layer manufacturing of titanium matrix composites using the direct metal deposition laser process [J]. Materials Science and Engineering A, 2016, 677: 171−181.

[25] VEIGA F, GIL DEL VAL A, SUÁREZ A, ALONSO U. Analysis of the machining process of titanium Ti6Al−4V parts manufactured by wire arc additive manufacturing (WAAM) [J]. Materials, 2020, 13(3): 766.

[26] WU Bin-tao, DING Dong-hong, PAN Zeng-xi, CUIURI D, LI Hui-jun, HAN Jian, FEI Zhen-yu. Effects of heat accumulation on the arc characteristics and metal transfer behavior in wire arc additive manufacturing of Ti6Al4V [J]. Journal of Materials Processing Technology, 2017, 250: 304−312.

[27] ALONSO U, VEIGA F, SUÁREZ A, ARTAZA T. Experimental investigation of the influence of wire arc additive manufacturing on the machinability of titanium parts [J]. Metals, 2019, 10(1): 24.

[28] SHIVA S, PALANI I A, MISHRA S K, PAUL C P, KUKREJA L M. Investigations on the influence of composition in the development of Ni−Ti shape memory alloy using laser based additive manufacturing [J]. Optics & Laser Technology, 2015, 69: 44−51.

[29] XU Tian-qiu, ZHANG Meng, WANG Jia-chen, LU Tao, MA Shu-yuan, LIU Chang-meng. Research on high efficiency deposition method of titanium alloy based on double-hot-wire arc additive manufacturing and heat treatment [J]. Journal of Manufacturing Processes, 2022, 79: 60−69.

[30] WU Bin-tao, PAN Zeng-xi, DING Dong-hong, CUIURI D, LI Hui-jun, FEI Zhen-yu. The effects of forced interpass cooling on the material properties of wire arc additively manufactured Ti6Al4V alloy [J]. Journal of Materials Processing Technology, 2018, 258: 97−105.

[31] ELMER J W, GIBBS G. The effect of atmosphere on the composition of wire arc additive manufactured metal components [J]. Science and Technology of Welding and Joining, 2019, 24(5): 367−374.

[32] CABALLERO A, DING Jia-luo, BANDARI Y, WILLIAMS S. Oxidation of Ti−6Al−4V during wire and arc additive manufacture [J]. 3D Printing and Additive Manufacturing, 2019, 6(2): 91−98.

[33] UWANYUZE R S, KANYO J E, MYRICK S F, SCHAFFÖNER S. A review on alpha case formation and modeling of mass transfer during investment casting of titanium alloys [J]. Journal of Alloys and Compounds, 2021, 865: 158558.

[34] FENG Xin, LIANG Yi-long, SUN Hao, WANG Shu. Effect of dislocation slip mechanism under the control of oxygen concentration in alpha-case on strength and ductility of TC4 alloy [J]. Metals, 2021, 11(7): 1057.

[35] NAYDENKIN E V, MISHIN I P, RATOCHKA I V, LYKOVA O N, ZABUDCHENKO O V. The effect of alpha-case formation on plastic deformation and fracture of near β titanium alloy [J]. Materials Science and Engineering A, 2020, 769: 138495.

[36] ZHOU Si-yu, ZHANG Jian-fei, WANG Jia-yin, YANG Guang, WU Ke, QIN Lan-yun. Effect of oxygen levels in tent shielding atmosphere on microstructural and mechanical properties of Ti−6Al−4V fabricated by wire arc additive manufacturing [J]. Journal of Materials Engineering and Performance, 2022, 31: 5269−5278.

[37] NASIRI-ABARBEKOH H, EKRAMI A, ZIAEI-MOAYYED A A. Effects of thickness and texture on mechanical properties anisotropy of commercially pure titanium thin sheets [J]. Materials & Design, 2013, 44: 528−534.

[38] NEEDLEMAN A, RICE J R. Limits to ductility set by plastic flow localization [M]//Mechanics of Sheet Metal Forming. Springer, 1978: 237−267.

[39] LI Zi-xiang, LIU Chang-meng, XU Tian-qiu, JI Lei, WANG Dong-hai, LU Ji-ping, MA Shu-yuan, FAN Hong-li. Reducing arc heat input and obtaining equiaxed grains by hot-wire method during arc additive manufacturing titanium alloy [J]. Materials Science and Engineering A, 2019, 742: 287−294.

[40] WANG Jian, LIN Xin, LI Jia-qiang, HU Yun-long, ZHOU Ying-hui, WANG Chong, LI Qiu-ge, HUANG Wei-dong. Effects of deposition strategies on macro/microstructure and mechanical properties of wire and arc additive manufactured

Ti6Al4V [J]. Materials Science and Engineering A, 2019, 754: 735−749.
[41] WASZ M L, BROTZEN F R, MCLELLAN R B, GRIFFIN A J. Effect of oxygen and hydrogen on mechanical properties of commercial purity titanium [J]. International Materials Reviews, 1996, 41(1): 1−12.
[42] CLARKE C F, HARDIE D, IKEDA B M. Hydrogen-induced cracking of commercial purity titanium [J]. Corrosion Science, 1997, 39(9): 1545−1559.
[43] MCQUILLAN M K. Phase transformations in titanium and its alloys [J]. Metallurgical Reviews, 1963, 8(1): 41−104.
[44] THOMPSON Y, POLZER M, GONZALEZ-GUTIERREZ J, KASIAN O, HECKL J P, DALBAUER V, KUKLA C, FELFER P J. Fused filament fabrication-based additive manufacturing of commercially pure titanium [J]. Advanced Engineering Materials, 2021, 23(12): 2100380.
[45] LÜTJERING G. Influence of processing on microstructure and mechanical properties of (α+β) titanium alloys [J]. Materials Science and Engineering A, 1998, 243: 32−45.
[46] CHAN W L, FU M W. Experimental studies and numerical modeling of the specimen and grain size effects on the flow stress of sheet metal in microforming [J]. Materials Science and Engineering A, 2011, 528: 7674−7683.
[47] WANG M, LI H Q, LOU D J, QIN C X, JIANG J, FANG X Y, GUO Y B. Microstructure anisotropy and its implication in mechanical properties of biomedical titanium alloy processed by electron beam melting [J]. Materials Science and Engineering A, 2019, 743: 123−137.
[48] NASIRI-ABARBEKOH H, EKRAMI A, ZIAEI-MOAYYED A A, SHOHANI M. Effects of rolling reduction on mechanical properties anisotropy of commercially pure titanium [J]. Materials & Design, 2012, 34: 268−274.
[49] SUN Lei, XU Zhu-tian, PENG Lin-fa, LAI Xin-min. Effect of grain size on the ductile-brittle fracture behavior of commercially pure titanium sheet metals [J]. Materials Science and Engineering A, 2021, 822: 141630.
[50] NIE Da-ming, LU Zhen, ZHANG Kai-feng. Grain size effect of commercial pure titanium foils on mechanical properties, fracture behaviors and constitutive models [J]. Journal of Materials Engineering and Performance, 2017, 26(3): 1283−1292.
[51] MIMOTO T, UMEDA J, KONDOH K. Titanium powders via gas−solid direct reaction process and mechanical properties of their extruded materials [J]. Materials Transactions, 2015, 56: 1153−1158.

力学性能可调的高氧钛原位电弧增材制造

李昌远[1]，刘长猛[1]，鲁 涛[1]，郭跃岭[1]，刘 彬[2]

1. 北京理工大学 机械与车辆学院，北京 100081；
2. 中国运载火箭技术研究院 北京宇航系统工程研究所，北京 100076

摘 要：通过电弧增材制造原位制备高氧钛，并对高氧钛的成分偏析、显微组织和力学性能进行研究。结果表明，高氧钛试样的显微组织主要呈现为针状 α 相集束。随着氧含量的增加，试样针状 α 相逐渐变宽，集束尺寸变大。受氧的强化作用以及晶粒尺寸效应共同影响，试样的强度先提高后下降，伸长率显著下降，断裂形式由塑性断裂向解理断裂过渡。当氧含量达到 0.37%(质量分数)时，伸长率约为 7%，试样抗拉强度超过 730 MPa，约为商业纯钛的 2 倍。

关键词：电弧增材制造；纯钛；高氧含量；显微组织；力学性能

(Edited by Bing YANG)